

A hot transient outflow from η Carinae

Ehud Behar¹, Raanan Nordon¹, Eyal Ben-Bassat¹, and Noam Soker¹

ABSTRACT

η Carinae (η Car) is a stellar binary system with a period of 5.54 years. It harbors one of the brightest and most massive stars in our galaxy. This paper presents spectroscopic evidence for a fast (up to 2,000 km s⁻¹) X-ray outflow of ionized gas launched from η Car just before what is believed to be the binary periastron (point of smallest binary separation). The appearance of this high-velocity component, just as the irregular flares in the X-ray light curve, can not be explained by the simple continuous binary wind interaction, adding to the intrigue of the η Car system.

Subject headings: techniques: spectroscopic — X-rays: stars — stars: mass loss — stars: individual: η Carinae

1. INTRODUCTION

Despite being studied for many years and in all wavebands, the η Carinae system (η Car), best known for its spectacular nebula (Morse et al. 1998) that can be tracked back to the Great Eruption of 1840 (Davidson & Humphreys 1997) is still much of a mystery. It is now believed to be a stellar binary system with a period of 5.54 years (Damineli 1996). The primary star is one of the brightest and most massive ($\sim 120 M_{\odot}$) stars in our galaxy. The system is currently in a phase of immense mass ejection. The X-rays detected from η Car can be explained by the collision of the two stellar winds (Corcoran et al. 2001a; Pittard & Corcoran 2002), not so the 70 day X-ray minimum observed periodically around periastron (Corcoran 2005).

Currently, the mass loss rate of the primary exceeds $10^{-4} M_{\odot}$ yr⁻¹ (Smith et al. 2003) and that of the secondary is an order of magnitude lower (Pittard & Corcoran 2002), but still unusually high. The wind of the secondary is much faster (few 1,000 km s⁻¹, Pittard & Corcoran 2002) than that of the primary (~ 600 km s⁻¹ and depending on latitude, Smith et al. 2003). The X-ray flux between 2 and 10 keV during the past 12 years is normally at a level of

¹Department of Physics, Technion, Haifa 32000, Israel. behar@physics.technion.ac.il (EB).

5×10^{-11} erg s $^{-1}$ cm $^{-2}$, as expected from the collision of the two stellar winds (Usov 1992; Corcoran et al. 2001a; Pittard & Corcoran 2002). The X-ray light curve is roughly constant throughout most of the 5.54 year orbital period, but rises gradually by a factor of 3–4 upon approach to periastron at which time short flares appear (Corcoran et al. 1997), before it drops sharply and stays in an X-ray low state (< 20% of normal brightness) for approximately 70 days. The full X-ray light curve can be found in Corcoran (2005). Although absorption by the dense primary wind may play a certain role in attenuating the X-ray emission from η Car, both spectral and temporal arguments have been put forward to reject absorption or an eclipse as the prime reason for this persisting low state (Hamaguchi et al. 2004; Soker 2005; Akashi et al. 2006), which is unique to η Car. Recently, it has been proposed that if the binary separation during periastron is small enough, the massive primary wind could smother the secondary wind and thus shut down the X-ray emission (Soker 2005; Akashi et al. 2006). However, so far there has been no direct evidence for accretion.

In this work, we wish to add to the temporal aspects of the η Car tale a high-resolution X-ray spectroscopic dimension. This is achieved by using five deep exposures of η Car with the High Energy Grating Spectrometer (HETGS) on board the *Chandra* X-ray Observatory (CXO), only the first of which has been published (Corcoran et al. 2001a,b). Theoretical variations of spectral line profiles in binary colliding wind systems have been modeled by Henley et al. (2003). The varying line profiles presented here for η Car, however, do not follow these models, at least not in a straightforward way, as we explain in §3.

2. Observations & Results

The log of the *Chandra* observations is given in Table 1. Two observations (3745 and 3748) coincide with the short intense flares just before periastron. The exact time of periastron is not well determined and depends on the uncertain orbital parameters of the system. Nonetheless, for the sake of presentation, we assume throughout this paper a period of 5.54 years (2024 days) and set phase zero to be at 2003-06-29. The X-ray low state, thus, occurs during phase 0 – 0.035. The data were retrieved from the CXO archive and processed using standard software (CIAO version 3.2.2.). *Chandra*'s HEG and MEG (high and medium energy gratings) spectrometers operate simultaneously in the 3.5 – 7.5 Å band of interest here and their spectra are consistent with each other. Aiming at the highest possible kinematic resolution, however, the higher spectral resolving power of the HEG in this band (factor of ~ 2) is favored over the slightly higher effective area of the MEG (factor of ~ 2), especially since the co-added plus and minus 1st order HEG data are already of sufficiently high signal-to-noise ratio (S/N).

To reveal the dynamics of the X-ray gas, we transferred each spectral line profile to line-of-sight velocity space (v_{\parallel} in km s^{-1}) using the simple non-relativistic Doppler shift $v_{\parallel} = c(\lambda - \lambda_0)/\lambda_0$, where λ and λ_0 represent the observed and rest-frame wavelengths of the line, respectively, and c is the speed of light. Negative and positive velocities represent approaching and receding gas, respectively. Fig. 1 shows the broad and variable X-ray line profiles observed in η Car as demonstrated on the Si^{+13} $\text{Ly}\alpha$ unresolved doublet at 6.18 Å. As expected, the MEG profile represents a smoothed version of the higher-resolution HEG profile. The observed line is much broader than the instrumental line spread function (also shown). Fig. 1 also demonstrates how the line profile varies dramatically from assumed phase $\phi = -0.470$ (Obs. 632) to $\phi = -0.028$ (Obs. 3745). The early-phase ($\phi = -0.470$) line is centered around zero velocity with no significant emission beyond 700 km s^{-1} (FWHM = $1000 \pm 100 \text{ km s}^{-1}$). The line closer to periastron ($\phi = -0.028$) features high velocity gas up to $\sim 2000 \text{ km s}^{-1}$. A gaussian fit yields a centroid shift of $-550 \pm 90 \text{ km s}^{-1}$, although the profile is clearly asymmetric.

In each observation, the kinematic profiles of all lines are fairly similar. This is demonstrated in Fig. 2, where we present four bright spectral lines from Obs. 3745 ($\phi = -0.028$). The profiles are unambiguously broad and asymmetric with approaching velocities reaching $2,000 \text{ km s}^{-1}$, but with no significant receding emission beyond $\sim 700 \text{ km s}^{-1}$. In order to understand how the line profiles vary between observations and as a function of phase we co-added the profiles of nine bright lines in each observation, namely the $\text{Ly}\alpha$ (1s-2p), $\text{He}\alpha$ resonance (1s²-1s2p) and $\text{He}\alpha$ forbidden (1s²-1s2s) lines of the Si, S, and Ar ions. Since the profiles of all these lines in a given observation are roughly similar (e.g., Fig. 2), co-adding gives an average profile with improved S/N. Individual Fe lines below 2 Å could not be included in this analysis, despite their high intensity, since the HETGS resolving power decreases strongly at these low wavelengths to the extent that the He-like Fe line complex is unresolved. The blue wing of the $\text{He}\alpha$ Fe resonance line is consistent with, though not resolved as well as, the other line profiles presented here. The resulting mean profiles have been normalized (except for Obs. 3747) to facilitate the comparison and are presented in Fig. 3. The observed, mean, unnormalized peak intensities for the assumed phases: -0.470 , -0.130 , -0.028 , -0.006 , and $+0.044$ are, respectively, 2.0 , 3.9 , 3.9 , 1.9 , and 0.3 , $\times 10^{-3} \text{ ph s}^{-1} \text{ cm}^{-2} \text{ \AA}^{-1}$. However, any interpretation of the *absolute* line fluxes in terms of the orbital parameters would be risky, as the observed variability is a result of both abrupt flaring and varying absorption.

A clear trend can be seen in Fig. 3. Far from periastron, the line profile is relatively symmetrical and narrow. Closer to periastron, bright components of gas moving towards us at velocities as high as $-2,000 \text{ km s}^{-1}$ start to develop. As the system further approaches periastron, the outflow dominates the line profile to the point where the bulk of the emission

is clearly blue-shifted. After periastron absorption considerably attenuates the emission lines to the low level seen in Fig. 3. Naive gaussian fits to the first two profiles yield centroids at $-25 \pm 25 \text{ km s}^{-1}$ (for $\phi = -0.470$) and at $-50 \pm 20 \text{ km s}^{-1}$ ($\phi = -0.130$) both with FWHM = $700 \pm 50 \text{ km s}^{-1}$. The late-phase asymmetric profiles are non-gaussian. For the mere purpose of quantifying the centroid shift, we performed two-gaussian fits, which yield peaks at $-120 \pm 50 \text{ km s}^{-1}$ and $-800 \pm 100 \text{ km s}^{-1}$ for $\phi = -0.028$ and at $-170 \pm 50 \text{ km s}^{-1}$ and $-1000 \pm 100 \text{ km s}^{-1}$ for $\phi = -0.006$. It is hard to rule out high-velocity *receding* gas before the X-ray minimum, since in agreement with Hamaguchi et al. (2004), we find that the column density toward the X-ray source rises from $5 \times 10^{22} \text{ cm}^{-2}$ long before periastron to $3 \times 10^{23} \text{ cm}^{-2}$ just after it. Emission from the far side of the system, thus, could be strongly absorbed.

3. Interpretation & Discussion

The colliding wind binary model, which is generally accepted for explaining the X-ray emission of η Car, has several clear predictions regarding the spectral line profiles expected at different orbital phases. The Doppler shifts are the result of shocked gas flowing along the contact discontinuity (CD) surface and away from the stagnation point (SP). If the shock opening angle is between $45^\circ - 90^\circ$ (Pittard & Corcoran 2002), the broadest line profiles are expected when the system is observed perpendicular to the line connecting the two stars, as the hottest gas formed around the SP flows directly towards and away from the observer. In this case, the lines are centered at zero velocity and are intrinsically symmetrical, but could be skewed by absorption of the far (red) emission. On the other hand, when the system is observed from behind one of the stars, shifted centroids are expected. If the system is observed from behind the weaker (stronger) wind, downstream shocked gas is flowing along the CD surface in the general direction of (opposite) the observer, producing blue- (red-) shifted centroids. The maximum velocities in this case would be less than those in the first (orthogonal) orientation. For a complete and detailed calculation of line profiles from colliding winds see Henley et al. (2003). In the following, however, we argue that the current line profiles observed at the different phases of the η Car orbit are in contradiction, even qualitatively, with the simple colliding wind scenario.

If the major axis of the η Car binary is perpendicular to our line of sight (Smith et al. 2004), the broadest profiles are expected at apastron (see above), but that is when the observed profiles are narrowest ($\phi = -0.470$). Also, with this geometry, the secondary would have to pass in front of the primary before periastron (in contrary to the picture of Smith et al. (2004)) to explain the blue-shifted centroids at $\phi = -0.028, -0.006$, but that would produce symmetrical (blue-shifted) profiles as absorption through the secondary wind

is weak, while strongly asymmetrical profiles are observed. In any case, the lower velocities observed near apastron appear to rule out this orientation if the colliding wind geometry is to produce the observed X-ray line profiles.

If alternatively, the projection of the line of sight on the orbital plane is more or less along the major axis and the viewing angle at apastron is from behind the secondary (Corcoran et al. 2001a), the observed blue-shifts at $\phi = -0.028, -0.006$ could be ascribed to gas flowing from the SP towards the observer and the unobserved red wing of the line to absorption by the primary wind. However, according to this scenario, at apastron one would expect blue-shifted centroids of at least a few 100 km s^{-1} due to downstream gas (see above), which is not observed ($\phi = -0.470$). For an observer above the binary plane ($i < 90^\circ$), as seems to be the case in η Car (Corcoran et al. 2001a), the problem becomes more severe (higher blue-shift is expected, but not observed).

In short, the observed behavior of the X-ray line profiles of η Car appear qualitatively inconsistent with a naive wind-collision scenario, since the interpretation of the high blue-shifts from a post-shock stream can not be made consistent with all phases. Henley (2005), comparing with line profiles calculated from hydrodynamical simulations, also reached the conclusion that the observed profiles are not as expected from simple models of the geometry of the wind-wind collision. He suggested that including the Coriolis effect may bring the models to better agreement with observations. Kashi & Soker (2007) suggest the effect of orbital motion, which can account for small centroid shifts, but can not explain the currently observed X-ray profiles. Here, we wish to propose an alternative explanation. In particular, we note that the asymmetric line profiles are observed during strong peaks in the X-ray light curve. These peaks too can not be accounted for by the simple colliding wind model (Pittard & Corcoran 2002; Henley et al. 2003), or by the Coriolis force.

We therefore prefer to interpret the observed high-velocity gas up to -2000 km s^{-1} in terms of a transient, collimated fast wind, or a jet, ejected from the immediate vicinity of the binary system through the interaction of the two stars. The peaks in the light curve hint that the outflow may be in the form of blobs. The unresolved *Chandra* images and the rapid variations both indicate that the outflow is restricted to within approximately $2 \times 10^{16} \text{ cm}$ from the center (assuming $0.5''$ at η Car's distance of 2.3 kpc). The appearance of the same charge states in the spectra attained during all phases implies that the temperatures of the X-ray gas and line-emitting outflow remain in the range of $kT = 2 - 5 \text{ keV}$. Consequently, we speculate that the fast component of the outflow consists of gas shocked by the collision of the winds (as observed throughout the orbit) that is launched and collimated near periastron. The widths of the major peaks seen in Figs. 2 and 3 suggest that the outflow is only moderately collimated to within $\sim 30^\circ$. The condensation of shocked gas provides a natural

explanation for the rise in X-ray intensity during the short intermittent flares observed in the X-ray light curve. A collimated outflow from the secondary has also been suggested to explain the enhanced He II $\lambda 4686$ emission before periastron (Soker & Behar 2006). Interestingly, both proper motion and Doppler shifts have been measured for high-velocity visible-light knots much further out from the center (Walborn et al. 1978; Meaburn et al. 1993). The optical knots were ejected more than a hundred years ago along the minor axis of the nebula (Meaburn et al. 1993). We would expect the present outflow to be launched along the major axis of the nebula although we have no pertinent information on its present direction with respect to the system’s geometry. If indeed that is the case and if the inclination angle of the binary plane to our line of sight is $i = 42^\circ$ (Smith 2002), the actual outflow velocity would be as high as $\sim 2,700$ km s $^{-1}$.

As the massive η Car primary is a short-lived star shedding considerable mass and as it is now understood that core collapse supernovae can not expel more than a few solar masses, implying that higher mass stars must shed most of their mass prior to the explosion, the winds and fast outflow of η Car may be a supernova in the making. At the very least, it highlights the next periastron passage on 2009, January 12 as a faithfully scheduled experiment for the astrophysically common, but poorly understood phenomenon of jet launching.

This research was supported by grant #28/03 from the Israel Science Foundation, and by a grant from the Asher Space Research Institute at the Technion.

REFERENCES

Aksah, M., Soker, N. & Behar, E. 2006, ApJ, 644, 451.

Corcoran, M. F., et al. 1997, Nature 390, 587.

Corcoran, M. F., Ishibashi, K., Swank, J. H. & Petre, R. 2001a ApJ, 547, 1034.

Corcoran, M. F., et al. 2001b, ApJ, 562, 1031.

Corcoran, M. F. 2005, AJ, 129, 2018.

Davidson, K. & Humphreys, R. M. 1997, Annu. Rev. Astron. Astrophys. 35, 1.

Damineli, A. 1996, ApJ, 460, L49.

Hamaguchi, K. et al. 2004 (astro-ph/0411271).

Henley, D. B., Stevens, I. R., & Pittard, J. M. 2003, MNRAS, 346, 773.

Henley, D. B., Ph.D. thesis, <http://www.physast.uga.edu/~dbh/thesis/>

Kashi, A. & Soker, N. 2007, astro-ph/0702661

Meaburn, J. et al. 1993, A&A, 276, L21.

Morse, J. A., et al., 1998, AJ, 116, 2443.

Pittard J. M. & Corcoran, M. F. 2002, A&A, 383, 636.

Smith, N. 2002, MNRAS 337, 1252.

Smith, N., Davidson, K., Gull, T. R., Ishibashi, K. & Hillier, D. J. 2003, ApJ, 586, 432.

Smith, N., Morse, J. A., Collins, N.R., & Gull, T. R. 2004, ApJ, 610, L105.

Soker, N. 2005, ApJ, 635, 540.

Soker, N. & Behar, E. 2006, ApJ, 652, 1563.

Usov, V. V. 1992, ApJ, 389, 635.

Walborn, N. R., Blanco, B. M. & Thackeray, A. D. 1978, ApJ, 219, 498.

Table 1. CXO/HETG Observation Log

CXO archive ID ^a	Start Time	Exposure (ks)	Assumed Orbital Phase (ϕ) ^b	2–10 keV Flux (10^{-10} erg s ⁻¹ cm ⁻²)
632	2000-11-19 02:46:40	90.69	−0.470	0.50
3749	2002-10-16 08:08:49	93.96	−0.130	0.98
3745	2003-05-02 11:56:16	97.29	−0.028	2.2
3748	2003-06-16 05:35:28	100.1	−0.006	0.97
3747	2003-09-26 22:45:53	72.16	+0.044	0.48

^aOne additional observation was carried out during the X-ray minimum (ID 3746 at 2003-07-20 01:46:22) for which no useful spectrum could be obtained.

^bPhase is approximated based on the assumption of a 5.54 year (2024 day) orbit, where phase zero is set at 2003-06-29 and the X-ray low state occurs during phase 0 – 0.035.

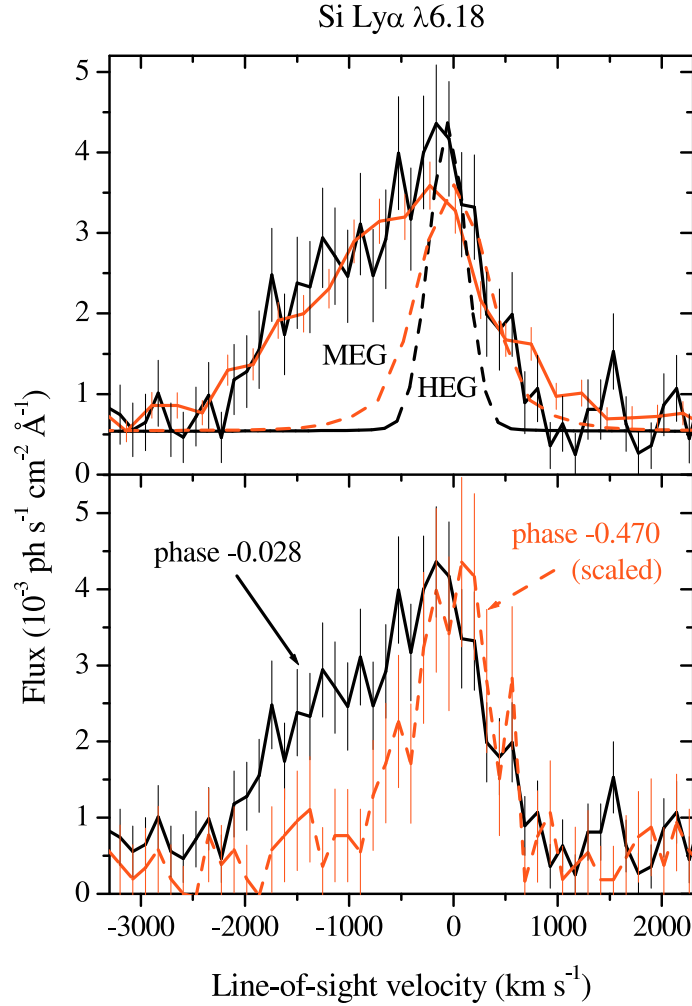


Fig. 1.— Velocity profiles of the Si $^{+13}$ Ly α unresolved doublet (6.180 and 6.186 \AA). *Upper panel* shows consistent HEG (higher spectral resolution) and MEG (smoother) data from Obs. 3745 ($\phi = -0.028$). The profile is clearly broadened up to 2000 km s^{-1} , much beyond the instrument line spread functions (dashed lines). *Bottom panel* shows the HEG profile of Obs. 632 ($\phi = -0.470$, dashed line) and Obs. 3745 ($\phi = -0.028$). The scaled up line from the early phase is rather symmetrical and much narrower, showing no line emission beyond 700 km s^{-1} .

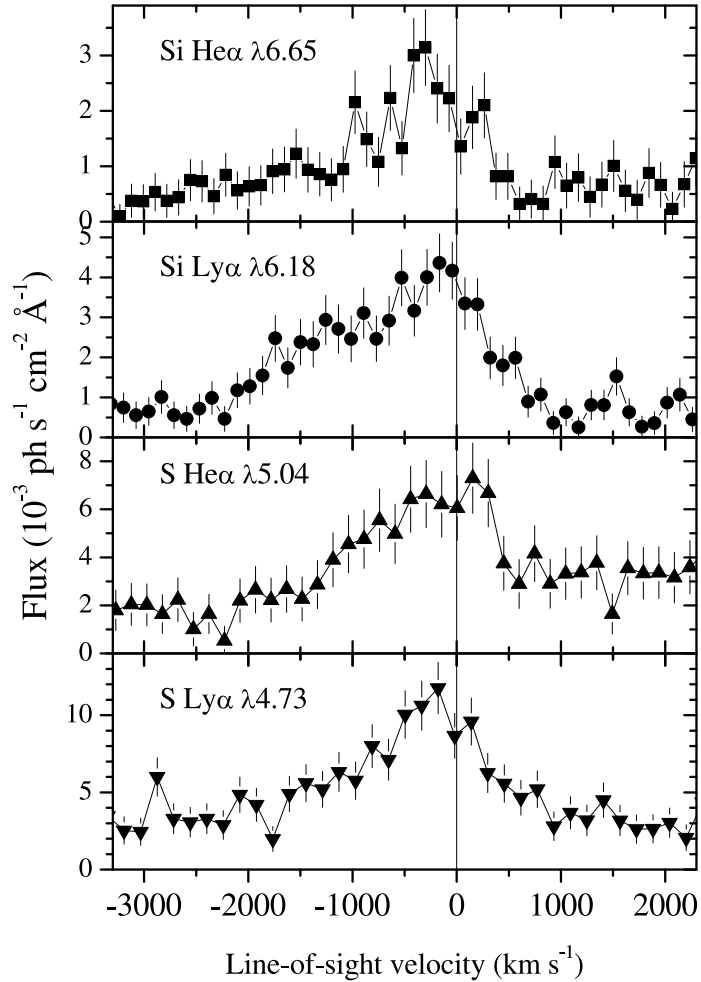


Fig. 2.— Profiles of four bright spectral lines from Obs. 3745 (assumed phase -0.028). The consistent asymmetric profiles with blueshifts up to $\sim -2,000$ km s⁻¹ are clearly seen.

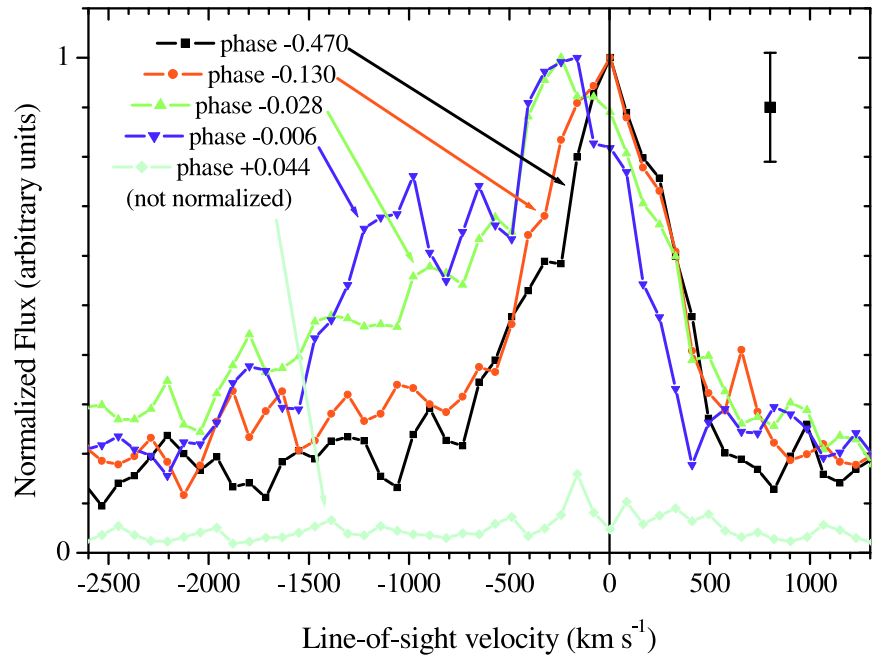


Fig. 3.— Mean, normalized, velocity profiles constructed from nine different spectral lines for the five observations of η Car. Only the profile of Obs. 3747 (assumed phase +0.044) during which η Car was strongly absorbed is not normalized and plotted at its correct scale with respect to Obs. 632 (assumed phase -0.470). Typical 1σ errors on each data point are 10 – 15 % (top right hand side).